

Research Article

Predicting Shear Capacity of FRP-Reinforced Concrete Beams without Stirrups by Artificial Neural Networks, Gene Expression Programming, and Regression Analysis

Ghazi Bahroz Jumaa^{1,2} and Ali Ramadhan Yousif³

¹Ph.D. Student, Department of Civil Engineering, Salahaddin University-Erbil, Erbil, Iraq

²Ass. Lecturer, University of Garmian, Kalar, Iraq

³Professor, Department of Civil Engineering, Salahaddin University-Erbil, Erbil, Iraq

Correspondence should be addressed to Ghazi Bahroz Jumaa; ghazijumaa@garmian.edu.krd

Received 29 July 2018; Accepted 18 October 2018; Published 15 November 2018

Guest Editor: Tayfun Dede

Copyright © 2018 Ghazi Bahroz Jumaa and Ali Ramadhan Yousif. This is an open access article distributed under the Creative Commons Attribution License, which permits unrestricted use, distribution, and reproduction in any medium, provided the original work is properly cited.

The shear strength prediction of fiber-reinforced polymer- (FRP-) reinforced concrete beams is one of the most complicated issues in structural engineering applications. Developing accurate and reliable prediction models is necessary and cost saving. This paper proposes three new prediction models, utilizing artificial neural networks (ANNs) and gene expression programming (GEP), as a recently developed artificial intelligent techniques, and nonlinear regression analysis (NLR) as a conventional technique. For this purpose, a large database including 269 shear test results of FRP-reinforced concrete members was collected from the literature. The performance of the proposed models is compared with a large number of available codes and previously proposed equations. The comparative statistical analysis confirmed that the ANNs, GEP, and NLR models, in sequence, showed excellent performance, great efficiency, and high level of accuracy over all other existing models. The ANNs model, and to a lower level the GEP model, showed the superiority in accuracy and efficiency, while the NLR model showed that it is simple, rational, and yet accurate. Additionally, the parametric study indicated that the ANNs model defines accurately the interaction of all parameters on shear capacity prediction and have a great ability to predict the actual response of each parameter in spite of its complexity and fluctuation nature.

1. Introduction

Although the behavior of steel-reinforced concrete (RC) members in shear has been extensively studied for more than one hundred years, and after numerous research challenges on shear behavior and on identification of the complex shear resistance mechanism of RC members, still there is an absence of comprehension and agreement on the mechanisms and behavior of shear resistance. While the behavior of steel-RC members in shear is an area of concern, the behavior of fiber-reinforced polymer-reinforced concrete (FRP-RC) members has additional complications due to their different mechanical properties [1]. Many important issues related to shear problems of FRP-RC members still remain without in-depth investigations and become open to discussion. Moreover, past investigations [2–4] inferred that the present shear design equations are exceptionally conservative in

predicting the shear capacity of FRP-RC beams. Consequently, the extra amount of FRP used to resist shear could be both costly and likely to create reinforcement congestion problems, and therefore, this study was motivated.

The shear strength of RC beams without web reinforcement was observed to be influenced by several variables, such as concrete strength (f'_c), shear span-to-depth ratio (a/d), beam depth (d), longitudinal reinforcement ratio (ρ_f), and beam width (b_w) [5, 6]. Additionally, for FRP-RC members, the type of FRP rebar and their variable mechanical properties, like low elastic modulus (E_f), high tensile strength, and low transverse shear strength, are other factors that should be taken into account.

Albeit many theoretical and empirical studies have been conducted to predict the shear strength of FRP-RC members, and to investigate the interaction between influencing parameters on shear strength mechanisms, up to date there is no

general agreement on a specific model. The vast majorities of the existing shear design equations have different forms and do not give a reliable factor of safety against shear failure; additionally, there is no general agreement between the existing codes and equations on the parameters affecting the shear capacity. This controversy in predicting models may be attributed to two main reasons; firstly, there is no comprehension theory on shear failure due to its complicated behavior and failure type which is sudden and catastrophic, and secondly, the existence wide variability in mechanical properties of FRP bars. Therefore, some existing predicting models were developed based on modifying the different theories which is originally proposed for steel-RC members and others are empirical or semiempirical models which were proposed based on a limited data; for instance, the ACI 440 algorithm was calibrated based on the test results from 326 steel-RC specimens and 44 FRP-RC specimens and the latter having a maximum effective depth of 360 mm. An alternative to classical and conventional methods for the prediction of complicated problems in various disciplines, such as the shear strength of FRP-RC members, is the utilization of artificial intelligence techniques like artificial neural networks (ANNs), fuzzy inference system (FIS), and genetic programming (GP). Throughout the most recent two decades, these methodologies have been prominent and effectively utilized as a part in an extensive variety of scientific applications particularly in civil engineering disciplines.

Recently, several studies have been performed on using different artificial intelligence techniques for predicting the shear capacity of FRP-RC members without stirrups. Kara [7] utilized gene expression programming (GEP) to obtain a simple model based on a set of 104 databases. Bashir and Ashour [8] suggested a model based on ANN using a set of 128 databases. Nasrollahzadeh and Basiri [9] developed an FIS to predict a model depending on a 128 database. Lee and Lee [10] used a database of 110 samples to propose a theoretical model utilizing ANN. Golafshani and Ashour [11] introduced a model using a new technique of biogeography-based programming based on an experimental database of 138 test specimens. Most of these studies proposed good models with a high level of accuracy; however, they used relatively a small size of a database. The size of the database used for training and testing the models plays a great role in the success of proposed models.

The present research aims to propose three new models to predict the shear strength, V_c , of FRP-RC slender beams without stirrups based on utilizing ANNs and GEP as artificial intelligence techniques and nonlinear regression analysis (NLR) as a conventional technique. These techniques were chosen due to the fact that the ANNs and GEP are powerful, accurate, and highly efficient tools in the model prediction of complicated problems, while the NLR is a classical tool which can be used to derive a simple, rational, and yet accurate model. The main affected parameters on shear strength are considered in modeling process which are f'_c , d , b_w , a/d , ρ_f , and E_f . The three models are derived using the largest collected database from the literature of (269) test specimens. The results of obtained models are compared to a large number of codes and proposed equations from the literature to examine their accuracy, validity, and efficiency. Additionally, a parametric study was conducted to indicate and compare the effect

of all parameters on shear capacity predicted by the proposed models and different well-known codes.

2. Reviews of Available Shear Design Equations

The last two decades witnessed development and rapid increase of using FRP-reinforcement for concrete structures; therefore, there are universal endeavors to create prediction models. These endeavors have brought about distributing a few codes and outline rules. However, there is no agreement in regards to shear configuration models among all available codes and guidelines. Table 1 provides a summary of the shear design equations for FRP-RC members without stirrups.

Most of the available shear design equations of FRP-RC members have been developed by modifying the existing equations adopted by design codes for steel-RC members. The methods of modification tried to cover the major changes in material properties by taking into account the effect of the lower elastic modulus, higher tensile strength, lower transverse shear strength, and no yielding criteria in the FRP rebar. Nevertheless, the relatively large variations in mechanical properties such as tensile strength, elastic modulus, bond properties, and transverse shear strength between the different FRP types have made it hard to precisely predict the shear capacity. Furthermore, the procedure that adopted by various codes, manuals, and guidelines to predict the shear strength are significantly different, and most of them are empirical and based on a limited set of test results. Consequently, some of the design models are quite conservative, whereas others sometimes yield unconservative results [3, 22]; as well as these equations are differing from each other in considered parameters. On the contrary, the design model that does not consider the effect of known parameters would lack generality, and its applicability to general design situations would be dubious [23]. Therefore, there is a need to develop shear design equations which will consider the effect of all parameters; as well as it will be accurate, consistent, and simple to use for the general application.

3. Collected Databases

For the purpose of this study, an extensive survey of the open literature was conducted and a large database containing the test results of a large number of 269 FRP-RC beams and one-way slabs were assembled. The database of the specimens were collected from 42 different references, reinforced with FRP rebars without transverse reinforcement, and only those that failed in the shear mode was compiled [1–3, 20, 22, 24–60]. Only slender beams and one way slabs with $a/d \geq 2.5$ were considered in this study. The specimens included 230 beams and 39 one way slabs; all were simply supported and were tested either under three points or four bending points. The details of the specimens that were used as a database are shown in Table 2.

4. Artificial Neural Networks (ANNs)

4.1. General Background. In its most broad frame, a neural network is a machine that is intended to demonstrate the

TABLE 1: Shear design equations for FRP-RC beams without stirrups.

Reference	Provisions
[12]	$V_c = (2/5)\sqrt{f'_c}b_w c$, $c = kd$, $k = \sqrt{2\rho_f n_f + (\rho_f n_f)^2} - \rho_f n_f$, $\rho_f = A_f/(b_w d)$
[13]	$V_c = \beta_d \beta_p \beta_n f_{vcd} b_w d / \gamma_b$; $f_{vcd} = 0.2(f'_c)^{1/3} \leq 0.72$ N/mm ² ; $\beta_d = (1000/d)^{1/4} \leq 1.5$; $\beta_p = ((100\rho_{fI} E_{fI})/E_s)^{1/3} \leq 1.5$ $\beta_n = 1.0$ for sections without the axial force, γ_b = member safety factor, $\gamma_b = 1.3$
[14]	$V_c = 0.79(100\rho_w(E_f/E_s))^{1/3}(400/d)^{1/4}(f_{cu}/25)^{1/3}b_w d$ ($100\rho_w(E_f/E_s)$) should not be taken greater than 3, and $(400/d)^{1/4}$ should not be taken if less than 1 for members with shear reinforcement
[15]	$V_c = 2.5\beta\phi_c f_{cr} b_w d_v$; $\beta = (0.4/(1 + 1500\varepsilon_x))(1300/(1000 + S_{ze}))$; $\varepsilon_x = (M_f/d_{v+V_f+0.5N_f})/(2(E_f A_f)) \leq 0.003$; $S_{ze} = ((35S_z)/(15 + a_g)) \geq 0.85S_z$, where $f_{cr} = 0.4\sqrt{f'_c}f_c \leq 69$ N/mm ² $V_c = 0.2\lambda\phi_c \sqrt{f'_c}b_w d \sqrt{E_{fI}/E_s}$
[16]	For sections with an effective depth greater than 300 mm, the concrete shear resistance, V_c , is taken as $V_c = (260/(1000 + d))\lambda\phi_c \sqrt{f'_c}b_w d \sqrt{(E_{fI}/E_s)} \geq 0.1\lambda\phi_c \sqrt{f'_c}b_w d \sqrt{(E_{fI}/E_s)}$; $\sqrt{(E_{fI}/E_s)} \leq 1.0$ Where λ = modification factor for density of concrete and ϕ_c = resistance factor for concrete $V_{Rd,ct} = 1.3(E_f/E_s)^{1/2}\tau_{Rd}k(1.2 + 40\rho_1)b_w d$ Satisfying the limitation: $1.3(E_f/E_s)^{1/2} \leq 1$ $V_{Rd,max} = 0.5vf_c b_w 0.9dv = 0.7 - f_c/200 \geq 0.5$ Where τ_{Rd} = design shear stress, MPa, defined as $0.25f_{ct}$; f_{ct} = characteristic tensile strength of concrete (5% fractile), MPa, $f_{ct} = 0.33\sqrt{f'_c}$; γ_c is the strength safety factor f concrete, $\gamma_c = 1.6$; k = factor taken equal to 1 in members where more than 50% of the bottom reinforcement is interrupted; if not, it will be $k = (1.6 - d) \geq 1 $; d = depth in meters; $\rho_1 = (A_f/b_w d)$ which cannot be taken less than 0.01 and greater than 0.02
[17]	$V_c = 0.05\lambda\phi_c k_m k_r (f'_c)^{1/3} b_w d_v$, $k_m = \sqrt{((V_f d)/M_f)} \leq 1.0$, $k_r = 1 + (E_f \rho_{fw})^{1/3}$ Such that $0.11\lambda\phi_c \sqrt{f'_c}b_w d_v \leq V_c \leq 0.22\lambda\phi_c \sqrt{f'_c}b_w d_v$, for $f'_c \leq 60$ MPa
[18]	In members with effective depth greater than 300 mm and with transverse reinforcement less than the minimum, V_c should be multiplied by $k_s = (750/(450 + d)) \leq 1.0$
[4]	$V_c = 2.1(((f'_c \rho_f d)/a)(E_f/E_s))^{0.3} b_w d$
[7]	$V_c = c_0/c_2 (\sqrt[3]{d/a} 100\rho_f (E_f/E_s) f'_c (c_1^2/c_0))^{1/3} b_w d$, $c_0 = 7.696$, $c_1 = 7.254$, $c_2 = 7.718$
[19]	$V_c = 0.045k_m k_r k_a k_s (f'_c)^{1/3} b_w d$, $k_m = ((Vd)/M)^{1/2}$, $k_r = 1 + (E_f \rho_f)^{1/3}$, $k_a = \begin{cases} 1 & \text{for } (M/(Vd)) \geq 2.5 \\ 2.5/(M/(Vd)) & \text{for } (M/(Vd)) < 2.5 \end{cases}$, $k_s = \begin{cases} 1 & \text{for } d \leq 300 \\ 750/(450 + d) & \text{for } d > 300 \end{cases}$
[1]	$V_c = ((0.2\lambda)/(a/d)^{2/3})((\rho_f E_f)/d)^{1/3} \sqrt{f'_c} b_w d$
[20]	$V_c = 2.76(\rho_{fI}(E_{fI}/E_s)(d/a)f'_c)^{1/3} b_w d$ $d \leq 300$ mm, $V_c = 2.76(\rho_{fI}(E_{fI}/E_s)(d/a)f'_c)^{1/3} (300/d)^{0.25} b_w d$ $d > 300$ mm
[21]	$V_c = v_c b_w d = ((0.134\sqrt{f'_c})/(\sqrt{1 + (d/(1.2d_c))}))b_w d$, $d_c = (\rho_w E(d_a + 16))/(100(a/d)\sqrt{f'_c})$

manner by which the brain plays out a specific errand or function; the system is generally executed by utilizing electronic parts or is mimicked in programming on an advanced PC. The ANNs perform helpful calculations and simulate complex modeling through a procedure of learning similar to that of the human brain. ANNs do not represent the sophistication, complication, and multifaceted nature of the brain, as the simulated neurons are substantially more straightforward than natural neurons in the area of recognition, efficiency, control, and learning. Nonetheless, ANNs are similar to the brain in two main points; first, the building squares of the two systems are straightforward computational tools which are exceedingly interconnected; second, the connections between neurons decide the task of the networks [61, 62].

ANNs are made out of numerous interconnected processing units operating in parallel. Each processing unit keeps some data locally, can play out some basic calculations, can have numerous input data and, however, can send just a single output. The ANNs have the ability to react and create the relating response and to adjust to the changing condition by learning from experience [63].

Generally, ANNs are trained, with the goal that specific input data prompt a particular target output. The network is balanced, in view of an examination of the output and the target, until the networks yield the objective. Gradually training the network modifies the weights and biases required after the introduction of every individual input vector. ANNs have been prepared to perform complex functions in different fields of application including biological, engineering, business, financial, manufacturing, medical, and military. Today ANNs can be prepared to tackle issues that are troublesome for regular PCs or human beings [64]. The drawback of the ANNs modeling is that it is not as simple as ordinary design provision, where it is consist of regularly numerous small units; therefore, simple calculations of the ANNs models are excessively monotonous, and usually, computers are needed for calculations.

4.2. Back Propagation ANNs. The multilayer perceptron, trained through the back-propagation algorithm, is nowadays the most broadly utilized neural networks. The term back propagation neural networks (BPNNs) alludes to

TABLE 2: Details of database.

Reference	Number of members	d (mm)	a/d	b (mm)	ρ_f (%)	f'_c (MPa)	E_f (GPa)	FRP type	V_{exp} (kN)
[24]	4	250	3	150	0.55–2.2	27.5–35	94	C	38.3–59.1
[27]	2	250–500	2.5	150–300	1.04	29.5–34	100	C	38.4–142.8
[26]	2	150	4	300	1.34–1.8	22.7–28	29.4	G	33.7–37
[25]	3	250	3	150	1.51–3.0	34.3	105	C	41.2–47.6
[28]	1	260	2.69	200	1.36	34.7	130	C	62.9
[29]	2	210	3.65	150	1.36	32.9–38.1	45	G	22.8–27.3
[30]	1	222	3.15	154	1.36	39	34	G	39
[31]	2	104–154	8.44–12.5	1000	0.49–0.76	66	41.3	G	42.1–85.2
[32]	5	157.5	4.5–5.8	305	0.73	27–30.8	40	G	28–30.9
[33]	3	279–287	2.61–2.69	178	0.77–2.3	24.1	40	G	36.7–54
[2]	18	225	4.06	178–254	1.11–2.27	36.3	40.3	G	28.1–51.1
[34]	2	258	2.5	150	0.91	53.8–68.5	48	G	38.5–41.4
[35]	6	360	3.39	457	0.96–1.92	39.9–42.6	37.6–47.1	A, G	94.8–177
[36]	12	225	4.06	152–203	1.25–2.56	79.6	40.3	G	30.4–48.3
[37]	11	310–346	2.75–3.71	130–160	0.72–1.54	34.1–43.2	42–120	G, C	42.7–52.3
[38]	11	143	6.36	89–159	0.33–0.76	60.3–81.4	139	C	8.8–23.1
[3]	6	225	2.67–4.5	200	0.25–0.88	40.5	145	C	36.1–47.2
[39]	1	970	3.14	450	0.46	40	40	G	136
[40]	2	190	7.96	121	1.1–1.65	40–74.3	40	G	13.9–16.9
[41]	8	159–165	6.06–6.49	1000	0.39–2.63	40	40–114	G, C	118–195
[42]	11	78–83	3.61–6.41	420	0.61–2.61	61–93	42	G	22.1–55.6
[22]	6	326	3.07	250	0.87–1.72	43.6–50	39–134	G, C	63–127.5
[43]	4	326	3.07	250	1.71–2.2	63	42–135	G, C	90–177
[44]	6	163–263	2.54–4.09	150	0.45–1.39	28.9–50.2	32	G	13.1–30.9
[45]	1	150	3.35	224	1.28	43	45	G	27.9
[46]	9	75	6–6.16	420	0.68–1.16	48–92	42	G	24.6–34.3
[47]	3	404–441	3.02–3.71	300	3.25–3.98	43	44–63	G	118.4–154.3
[48]	2	262	6.68	600	0.77–1.53	68	48	G	91.2–118.2
[49]	4	170	4.12	150	0.92–1.54	20–26.6	46	G	12.7–15.4
[50]	4	170	5.88	150	1.33–2.22	20–26.6	113	C	19.3–27.7
[51]	6	194–937	3.26–3.93	450	0.51–2.54	35–46	37	G	74–232
[52]	6	200–500	3.5–6.5	300	0.28–0.35	52.3	114	C	54.1–71.2
[53]	6	291–594	2.5	250–300	0.42–1.37	65.3–74.2	46.3–144	G, C	71.6–155.2
[54]	13	146–883	3.13	114–457	0.6–1.17	29.5–59.7	41–43.2	G	17.9–264.8
[1]	8	305–744	2.5	250–300	0.42–0.91	34.5–44.7	47–144	G, C	61–138.5
[55]	9	140	6.2	1000	0.52–1.25	41.3–86.2	140–144	C	118.5–192
[56]	34	216	2.5–4.5	150–200	0.33–0.79	30	48–148	G, C	16.9–35.4
[57]	3	150	4–4.5	245–270	0.39–0.85	60	70	B	20.9–29.2
[20]	6	170–370	2.7–5.9	200	0.12–0.52	22.1–28.7	141.4	C	17.6–36.1
[58]	6	170	5.65–7	300	0.8–4.1	35.9	48–53	B	29.3–51.5
[59]	8	206–220	2.5–3.3	152	0.31–1.52	49	50	B	17–30
[60]	12	234–635	2.6	200	0.71–2.69	42.2–73.4	58	B	54–169.5
Mean		258.8	4.13	290.4	1.123	46.2	73.8		58.8
Standard deviation		157.2	1.51	220.5	0.7290	18.19	42.93		48.44
Minimum		73	2.5	89	0.12	20	29.4		8.8
Maximum		970	12.5	1000	4.121	93	147.9		232

the way in which the gradient is processed for nonlinear multilayer networks [64]. The BPNNs algorithm follows a technique to minimize the errors through the calibration of the weights in each cycle by a small amount for a specific training scheme.

BPNNs is one of the straightforward and most appropriate networks being utilized in the prediction of civil engineering problems [63, 65, 66], principally because of that it can modify the weights of each layer in view of the errors introduced at the output. A common structure of BPNNs display comprises of an input layer, at least one hidden layer and an output layer, and each layer comprises

of many neurons. Every neuron is a processing unit that gets at least one source of input and produces an output response through the transfer function. Related to every connection is a weighting that communicates the impact on the present procedure component of an information set or another procedure component in the past layer, as shown in Figure 1. The connection weighting and bias values are at first picked as arbitrary numbers and afterward settled by the consequences of the training procedure [67].

The calculations that carried out inside the BPNNs include summation process of weighted input values with the

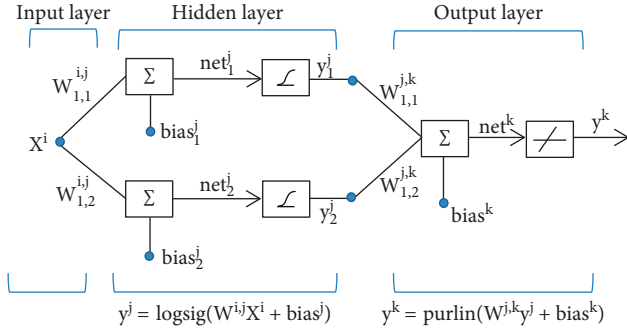


FIGURE 1: Typical architecture and log-sigmoid function of (1-2-1) BPNNs.

bias of the input layer, as in Equation (1), and then the results passed into the hidden layer neurons. Inside neurons, the process of sigmoid transformed function was performed by using one of the transformed functions such as that in Equation (2). Another linear process, using the purelin function, was carried out by summing the weighted output from the hidden layer neurons with the bias of the hidden layer as in Equation (3):

$$\text{net}_j = \sum_{i=1}^n w_{ij}x_i + \text{bias}_j, \quad (1)$$

$$y_j = f(\text{net}_j) = \frac{1}{1 + \exp^{-(\text{net}_j)}}, \quad (2)$$

$$y_k = \text{purelin}\left(\sum_{j=1}^m w_{jk}y_j + \text{bias}_k\right), \quad (3)$$

where net_j is the weighted sum generated at the j th hidden neuron; x_i is the input value from the i th input neuron; w_{ij} and w_{jk} are the weights added to the hidden layer and the output layer neurons, respectively; bias_j and bias_k are the biases added to the hidden layer and the output layer neurons, respectively; y_j is the processed output from the j th hidden neuron; y_k is the processed output from the k th output neuron; and n is the number of input neurons, and m is the number of neurons in the hidden layer.

4.3. BPNNs Model Used for the Prediction of Shear Capacity.

In this study, the BPNNs were utilized to produce a predictive model for shear strength of FRP-reinforced concrete members without stirrups. The key parameters affecting the shear strength which considered in this study are f'_c , d , b_w , a/d , ρ_f , and E_f . The most important issue in BPNNs modeling is selecting the number of hidden layers and the number of neurons in each hidden layer, which depend on several factors like type of problem of interest, the association of input parameters with the output pattern, size of instances, number of input parameters, and number of outputs. However, there is no basic acknowledged criteria to pick the number of hidden layers and the number of

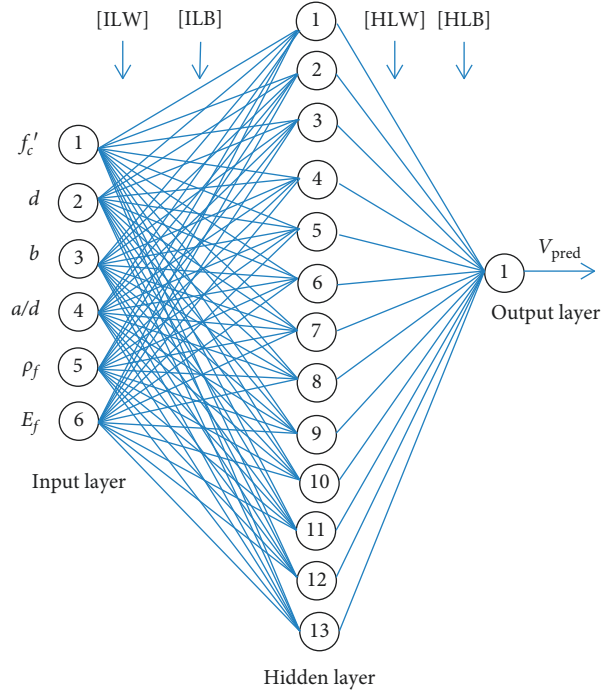


FIGURE 2: Architecture of BPNNs used for the prediction of the shear strength.

neurons; therefore, a trial and error method was achieved based on training and testing up to obtain a reasonable fit. Consequently, a BPNNs training algorithm was utilized in a feed-forward network trained using nonlinear hyperbolic log-sigmoid transfer function in the hidden layer and a linear purelin transfer function in the output layer, as in Equations (1)–(3).

The trial and error procedure resulted in that the best fitting model was that obtained using thirteen neurons in a single hidden layer (6-13-1), as demonstrated in Figure 2. The predictive model was trained through numerous iterations to find the best epoch value, momentum rate, and learning rate which give the optimum model for shear strength prediction. The data were divided arbitrarily into “training” 70%, “validating” 15%, and “testing” 15%, and the partitioning of data was chosen based on the results of model performance after numerous trials.

It is recommended by many authors [11, 63, 68, 69] to normalize the input and output data before using them to predict the model. In this study, the data of input and target were scaled by the linear normalization function in the range of (0 to 1), as shown in the following equation:

$$x_n = 0.6 \frac{x - x_{\min}}{x_{\max} - x_{\min}} + 0.2, \quad (4)$$

where x is the data sample, x_n is the normalized data sample, x_{\min} and x_{\max} is the minimum and maximum values of the data for the interested parameter.

The input layer weights (ILWs), the input layer biases (ILBs), the hidden layer weights (HLWs), and the hidden layer bias (HLB) of the (6-13-1) predictive BPNNs model are shown below:

$$\begin{aligned}
 ILW &= \begin{Bmatrix} -2.3567 & 0.27166 & 1.4696 & -1.4038 & 0.99307 & 2.2234 \\ 2.3842 & -2.2831 & 0.83159 & 2.2855 & 1.4806 & -0.83455 \\ 2.8211 & 0.75441 & -4.086 & 1.4427 & 1.7982 & -1.0877 \\ 0.59955 & -0.74937 & 2.0882 & -2.6609 & 1.8418 & -1.5433 \\ 1.4527 & -1.7869 & -1.0477 & 1.6872 & -0.81981 & -2.5634 \\ 3.5416 & -1.9591 & -0.34353 & 1.0741 & -1.5276 & 2.2139 \\ 1.5643 & -2.8231 & 2.6211 & -1.6244 & 1.0879 & 1.7129 \\ 2.2825 & -0.40079 & 0.48425 & -2.312 & 0.07062 & 0.15858 \\ -1.749 & -0.25004 & -0.45657 & -2.2347 & -1.0796 & -1.0232 \\ -0.78404 & 2.66 & -2.8673 & -1.0803 & -0.86988 & -1.6247 \\ -0.25678 & -3.2562 & 2.2726 & 1.6206 & -1.2616 & 2.6619 \\ -1.2662 & -0.78168 & -0.52983 & -2.5791 & 1.0124 & 2.3284 \\ -2.3043 & 0.55942 & -1.2328 & -2.8413 & -1.3658 & 2.6415 \end{Bmatrix}, \\
 ILB &= \begin{Bmatrix} 5.1888 \\ -1.4396 \\ -2.1773 \\ -2.4823 \\ -1.6444 \\ -0.08813 \\ 0.12198 \\ 2.2041 \\ -2.362 \\ -1.9906 \\ -0.52466 \\ -3.7706 \\ -2.6641 \end{Bmatrix}, \\
 HLW &= \{-0.7663 \ 1.2834 \ -0.9729 \ -0.66761 \ -0.3835 \ -0.87847 \ 1.2312 \ 1.3464 \ -1.3058 \ 1.206 \ 1.169 \ -0.9465 \ -0.6511\}, \\
 HLB &= \{-0.44036\}.
 \end{aligned}
 \tag{5}$$

5. Genetic Programming

5.1. General Background. Genetic programming (GP) is a naturally inspired machine learning (evolutionary) technique utilized for randomly reproducing a population of computer programs in light of Darwin's advancement hypothesis. GP, which was developed by Koza [70], can be regarded as a developed form of the genetic algorithm (GA), which is an evolutionary optimization tool that depends on the principles of genetics and normal determination. The systems of GA incorporate altering and changing the extent of chromosomes by genetic operators to solve function optimization problems. The fundamental contrast amongst

GA and GP is that the solution of GA is a binary string of fixed length utilized for parameters optimization of a specific arrangement of model parameters, while the solution of GP is a development program represented as a subset of parse trees which use input variables and corresponding outputs for generating optimized models [71–73].

The GP techniques for modeling incorporate production of an initial population of chromosomes (models) which include an arrangement of functions and an arrangement of terminals that selected and arranged randomly in the form of the parse tree (computer model). The models composed of a root node, functional nodes, and terminals, as shown in Figure 3.

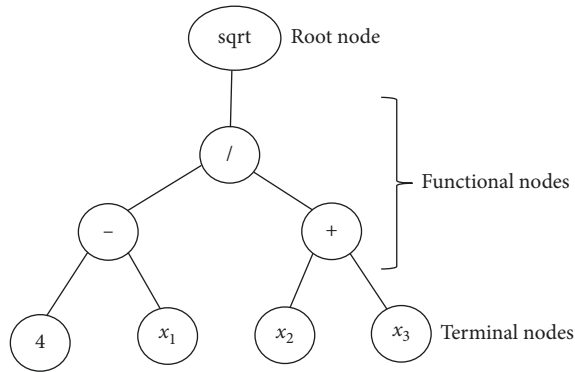


FIGURE 3: Typical example of a GP tree representation model $((4 - x_1)/(x_2 + x_3))^{1/2}$ [74].

At that point, the produced population models are assessed and the fitness of the models is evaluated using the provided data of the particular problem. After that, other generations of models are produced by primary genetic operators: reproduction, crossover, and mutation, as shown in Figure 4. The evolutionary procedure of assessing the fitness of the present population and producing new population is continued until the point when an end termination criterion is approached, which can be either a particular acceptable error or a specified maximum number of generations. The model with the best solution which developed after each generation assigns the outcome of the GP program [76].

5.2. Gene Expression Programming. The most widely used GP in civil engineering problems is gene expression programming (GEP), which was developed by Ferreira [71]. GEP utilizes development of numerical conditions that is encoded linearly in chromosomes of a consistent length and considered nonlinearly as expression trees (ETs) with various shapes and sizes. The chromosomes are composed of several genes; each gene contains a smaller subprogram or subexpression trees (Sub-ETs). Every gene has a consistent length and comprises a head and a tail. The schematic of the GEP flowchart is shown in Figure 5. The implementation of GEP predictive modeling incorporates five main components including function set, terminal set, fitness function, control parameters, and termination condition [7, 75].

The preferred quality of GEP is that the genetic operators work at the chromosome level and the production of genetic diversity is to a great degree simplified. Another favorable position is credited to the remarkable multigenetic nature of GEP, which permits the advancement of all the more capable models made out of a few subprograms [71].

5.3. GEP Model for Predicting Shear Capacity. For predicting the shear strength of FRP-reinforced concrete beams without stirrups by GEP-based formulation, six influencing parameters were considered: f'_c , d , b , a/d , E_f , and ρ_f , through training and testing the experimental results. The data are evaluated on the GeneXproTools 5 [78] to develop the empirical model which is the most widely used software for

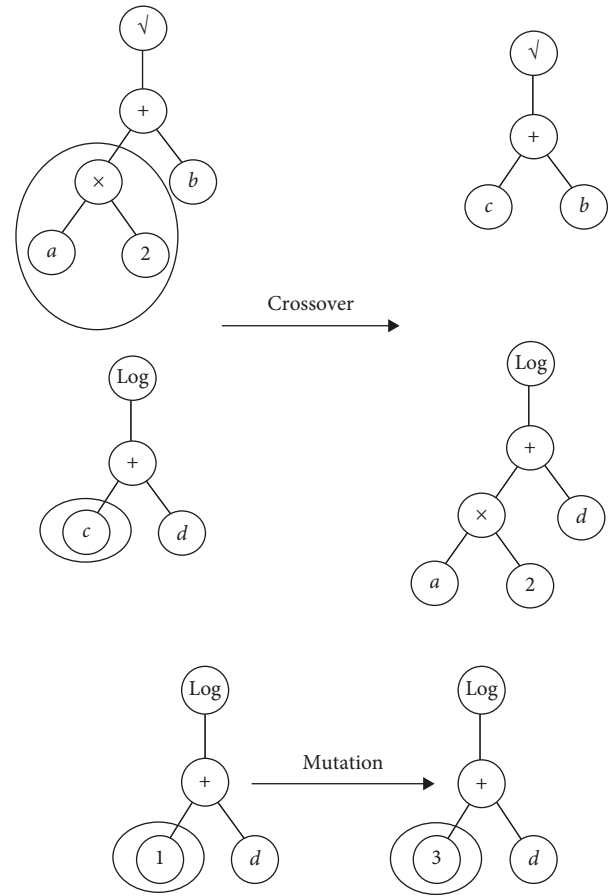


FIGURE 4: Typical operations of crossover and mutation in GP [75].

GEP model prediction. Similar to the ANNs model, the data are partitioned randomly to 70% for training and remaining 30% for testing such that both portions of data have balanced statistical parameters like mean, standard deviation, and max and min values.

To obtain the best GEP prediction model, many models with a different number of genes were evolved throughout a set of genetic operators (mutation, transposition, and crossover). Initially, a model composed of two genes with multiplication linking functions and head sizes of three was selected and evolved many times. Then, the model parameters were changed, step by step, through increasing the number of genes, head size, number of chromosomes, and weights of function sets. The program was evolved numerous times for various models, and the outcome models were monitored and compared to evaluate their performance. Other parameters like mutation rate, inversion, and points of recombination were chosen based on previous works [7, 79–82] and then evaluated to get their optimum effects. After many trials, the final mathematical model was chosen, for which the utilized parameters, fitness function, and function sets are given in Table 3. The final model was selected based on criteria of the best fitness and less complicity of mathematical formulation; the expression trees are shown in Figure 6 and the mathematical formulation is given in the following equation:

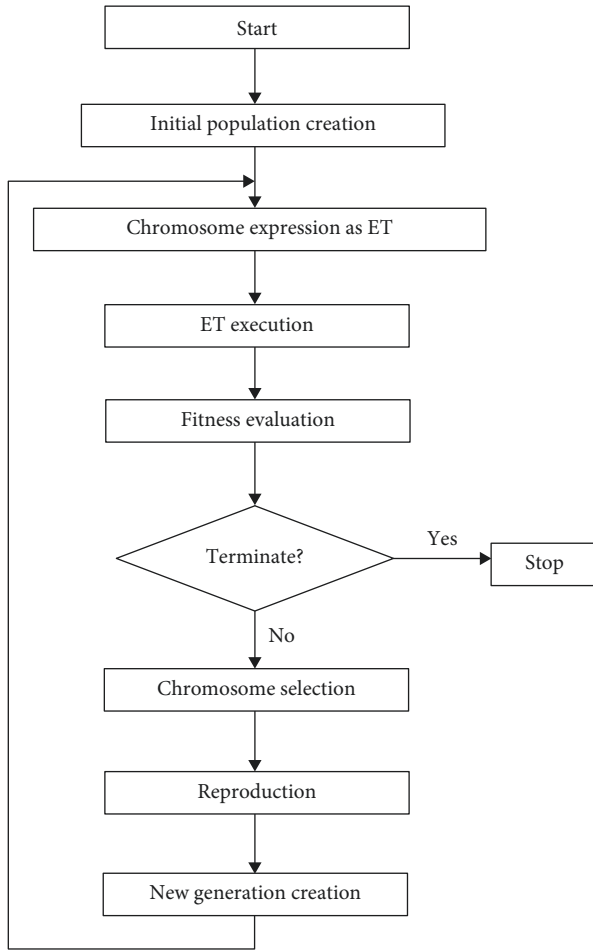


FIGURE 5: Flowchart of GEP [77].

$$\begin{aligned}
 V_c = & \left\{ \text{abs} \left(\left(\frac{c_3 + (d_5 * d_3)(d_2 + d_0)^2}{4} \right)^{1/3} \right) \right\} \\
 & * \left\{ \left(\tanh \left(\left(\frac{d_2}{d_1} \right)^{1/5} \right) - \tanh((d_2 * d_3)^4) \right)^5 \right\} \\
 & * \left\{ d_2 + \left(\frac{d_3^{1/5}}{\max(d_1; c_6)} (c_8 + d_4) \right)^2 \right\} \\
 & * \left\{ \left(\tanh \left(\left(\frac{d_2}{d_1} \right)^{1/5} \right) - \left(\sqrt{\frac{d_1}{d_0}} \right)^3 \right)^5 \right\},
 \end{aligned} \quad (6)$$

where: $d_0, d_1, d_2, d_3, d_4,$ and d_5 refer to $d, a/d, b, \rho_f, f'_c,$ and E_f respectively, $c_2 = 6.56723946184092$, $c_3 = -241413.053630399$, $c_4 = -12.1479701959083$, $c_6 = 3.07014791103389$, and $c_8 = 22.0241396443835$.

6. Nonlinear Regression Model (NLR)

Regression analysis is considered as an important tool that can be used in the modeling process for solving complicated problems of various engineering disciplines.

TABLE 3: Parameters used in the GEP Model.

Parameters	Values
Number of chromosomes	30–500
Head size	3, 5, 8
Number of genes	2, 3, 4
Linking function	Multiplication
Function set	$+, -, /, *, \text{abs}, \tanh, x^2, x^{1/2}, x^{1/3}, x^{1/5}, \dots$
Generation without changes	2000
Number of tries	12
Maximum complexity	10
Fitness function	RMSE
Mutation	0.044
Inversion	0.1
One-point recombination	0.3
Two-point recombination	0.3
Gene recombination	0.1
Gene transposition	0.1
IS transposition	0.1
RIS transposition	0.1
Data type	Floating point
Constants per gene	10

However, the proposed models based on nonlinear regression (NLR) are less accurate than the ANN and GEP; however, it is characterized by that it is simple and easy for application without the need of computers for calculations. A nonlinear regression model based on the experimental database collected from the literature was suggested. The proposed equation was derived based on developing a model similar to that proposed by Zsutty [83] which is the most accurate and simple empirical equation that was proposed for shear prediction of steel-RC members. In order to predict the shear strength of FRP-RC beams more accurately, considering the effect of all influencing parameters, the experimental shear strength was analyzed with most common influencing parameters: $f'_c, d, b, a/d, E_f,$ and ρ_f . Based on data fitting analysis, and after some simplification, the following equation was proposed:

$$V_c = 0.32 \left(\frac{1}{d} \right)^{1/3} \left(\frac{E_f \rho_f}{a/d} \right)^{2/5} (f'_c)^{1/5} b_w d. \quad (7)$$

It can be observed that the equation is simple, rational, and more generalized than most codes and proposed equations from the literature as it considers the effect of all the influencing parameters on the shear strength of FRP-RC members without stirrups.

7. Results and Discussion

The shear strength results of FRP-reinforced concrete members for the three proposed models, the ANNs, GEP, and NLR, are evaluated and compared with the common design provisions (ACI 440-15, JSCE-97, CSA 806-12) and seven proposed equations [1, 4, 7, 10, 19–21]. The comparison was examined based on statistical terms such as

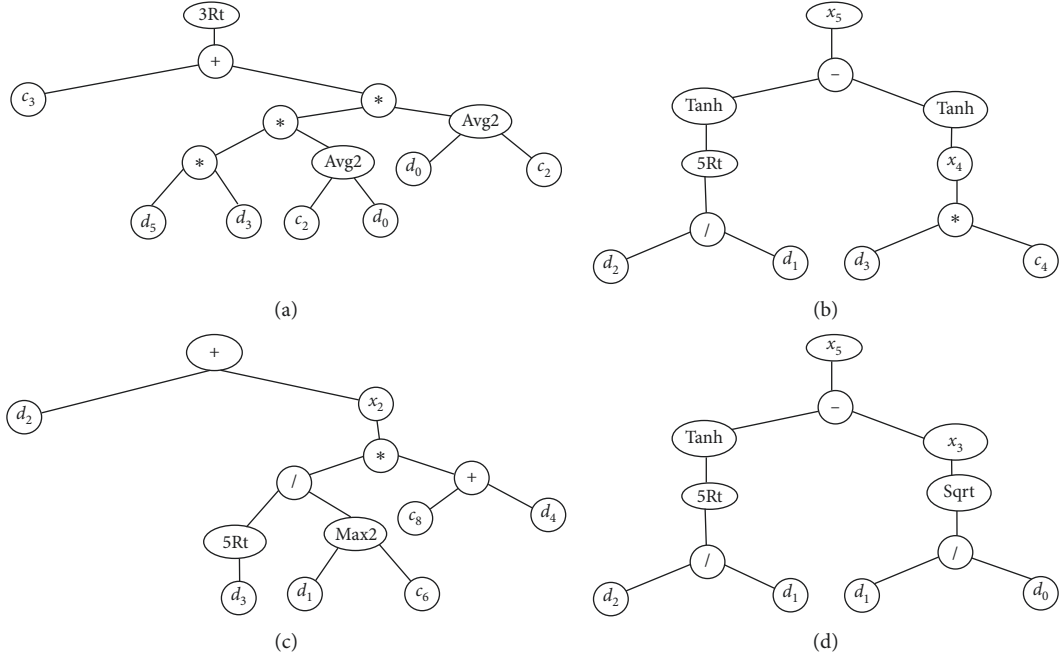


FIGURE 6: Expression trees ETs for the GEP model. (a) Sub-ET 1. (b) Sub-ET 2. (c) Sub-ET 3. (d) Sub-ET 4.

mean, standard deviation (SD), and coefficient of variation (COV) in addition to error values, such as mean absolute error (MAE), root mean square error (RMSE), and R^2 , as shown below:

$$\begin{aligned} \text{RMSE} &= \sqrt{\frac{\sum_{i=0}^N (e_i - p_i)^2}{N}}, \\ \text{MAE} &= \frac{1}{N} \sum_{i=0}^N |e_i - p_i|, \\ R^2 &= 1 - \frac{\sum_{i=0}^N (e_i - p_i)^2}{\sum_{i=0}^N (e_i - \bar{e})^2}, \end{aligned} \quad (8)$$

where e_i and p_i are the experimental and predicted shear force in kN, respectively, \bar{e} is the average of the experimental values, and N is the total number of the considered samples. The model that minimized the error values (MAE and RMSE) and maximized R^2 is selected as the optimum model.

Figure 7 presents the scatter of the experimental shear force, V_{exp} , versus the predicted shear strength, V_{pred} , for the proposed models, codes, and proposed equations from the literature. It is clear that the best models for predicting the shear strength are those suggested in this study, which in a sequence are ANNs, GEP, and NLR, as these models predict the shear strength very accurately with the optimum statistical performance of R^2 , RMSE, and MAE. High correlation coefficients with low error rates indicate that the proposed three models are excellent models and exhibit generalization performance in predicting shear strength of FRP-reinforced concrete beams without stirrups. In contrast, the code design provisions and other proposed equations from the literature yielded dispersion results with

lower R^2 and larger error rates as given in the scatter relationships.

Table 4 presents the statistical parameters (mean, standard deviation (SD), coefficient of variation (COV), minimum, maximum, range, RMSE, MAE, and R^2) of the ratio of experimental shear strength to the predicted shear strength, $V_{\text{exp}}/V_{\text{pred}}$, for the proposed models in this study, seven well-known codes, and seven proposed equations from literature based on the (269) collected database. It is clear that the proposed equations yielded superior accuracy between all the codes and proposed equation from the literature because their optimum statistical parameters such as the mean, SD, range, RMSE, and R^2 are 0.998, 0.113, 0.72, 5.3, and 0.9877, respectively, for ANNs; 1.007, 0.162, 0.88, 8.2, and 0.970, respectively, for GEP; and 1.003, 0.174, 0.99, 10.7, and 0.95, respectively, for NLR.

The ANNs and GEP models are artificial intelligent models derived based on soft computing; as verified above, these models are accurate, superior, and highly efficient in predicting the complicated problem such as shear strength. However, the drawback of artificial intelligent models is that it cannot be calculated manually and it needs computers for calculation. Besides, it is considered as a powerful and efficient tool which can be used in soft programs specialized for analysis and design of reinforced concrete structures. On the contrary, the NLR model is simply accurate and rational which can be used manually with sufficient accuracy more than the design codes and previously proposed equations. Nevertheless, the regression equations cannot properly define, with the same level of efficiency of artificial intelligent techniques, the interactions between the input and output parameters due to that the regression models usually are produced based only on a few predefined equations [79].

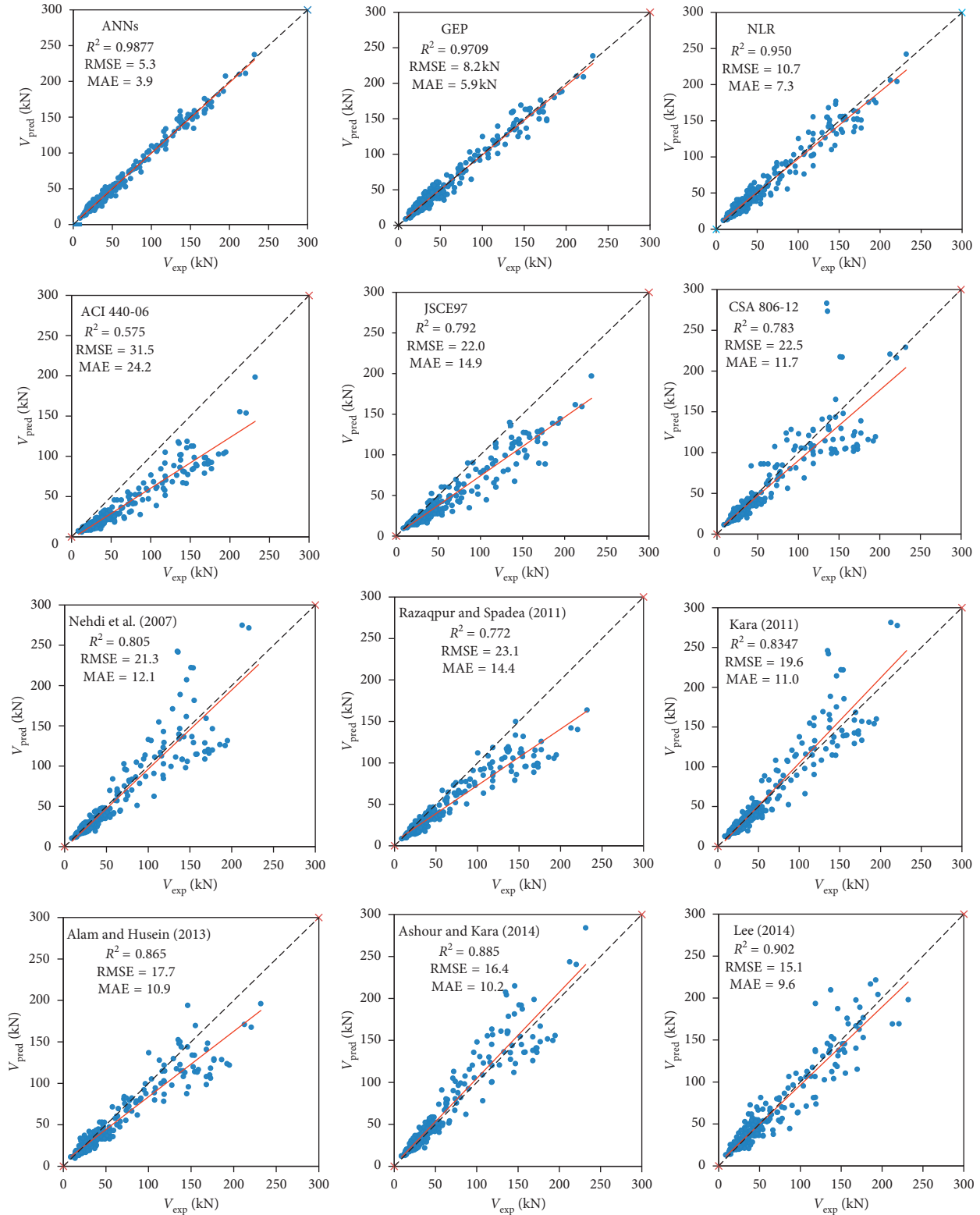


FIGURE 7: Scatter of V_{exp} versus V_{pred} for ANN, GEP, NLR, and different models from the literature.

Finally, it can be said that all the three proposed equations can be considered as accurate, efficient, and useful models, which were trained on a largest collected database, for predicting the shear strength of FRP-reinforced concrete members.

8. Parametric Analyses

For further verification of the proposed ANNs, GEP, and NLR prediction models, a parametric analysis was performed in this study. The main goal was to find the

TABLE 4: Statistical parameters of (V_{exp}/V_{pred}) for the proposed models and different design equations.

Design equations	Mean (V_{exp}/V_{pred})	SD	COV%	Minimum	Maximum	Range	RMSE	MAE	R^2
[12]	1.813	0.416	23.06	1.13	3.74	2.61	31.5	24.2	0.575
[13]	1.302	0.282	21.63	0.46	2.51	2.05	22.0	14.9	0.792
[18]	1.091	0.227	20.85	0.47	1.85	1.37	22.5	11.7	0.783
[16]	1.193	0.386	32.49	0.44	2.48	2.03	26.33	17.58	0.703
[17]	0.948	0.265	27.99	0.39	1.74	1.34	22.57	14.03	0.782
[14]	1.072	0.247	23.1	0.54	1.92	1.38	14.70	9.80	0.908
[15]	1.393	0.254	18.35	0.70	2.48	1.78	24.56	16.61	0.742
[4]	1.113	0.219	19.67	0.55	1.92	1.36	21.3	12.1	0.805
[19]	1.305	0.235	18.01	0.84	2.14	1.29	23.1	18.4	0.772
[7]	1.025	0.205	20.03	0.54	1.91	1.36	19.6	11.0	0.835
[1]	1.148	0.227	19.81	0.59	1.72	1.13	17.7	10.9	0.865
[20]	0.965	0.174	18.06	0.63	1.68	1.05	16.4	10.2	0.885
[10]	1.015	0.229	22.51	0.53	1.96	1.43	15.1	9.6	0.905
[21]	1.096	0.283	25.87	0.56	2.12	1.56	19.15	11.80	0.843
NLR	1.003	0.174	17.32	0.62	1.61	0.99	10.7	7.3	0.950
GEP	1.007	0.162	16.08	0.66	1.55	0.88	8.2	5.9	0.9709
ANNs	0.998	0.113	11.31	0.71	1.44	0.72	5.3	3.9	0.9877

response of the three proposed models to predict the shear strength for a set of input parameters which are selected taking into account the average value of each parameter in the collected database. For further showing the performance of the proposed models and for comparison purpose, the response of three well-known codes (ACI 440-15, JSCE-97, and CSA S806-12) was also considered. The approach depends on keeping all input parameters at their selected values, except that, in each time, a single parameter value was changed incrementally within the expected practical values. Consequently, an arrangement of manufactured data for the single considered parameter is produced; this procedure was repeated for all parameters so that all models are examined for the entire input parameters. The selected input parameters are $f'_c = 46$ MPa, $b_w = 200$ mm, $d = 400$ mm, $a/d = 4$, $\rho_f = 0.011$, and $E_f = 74$ GPa. It is worthy to note that the ANNs model cannot properly predict the shear strength for input parameters outside the range of training data; therefore, it is only valid for prediction within the range of input parameters of the training data [8].

Figure 8 indicates the tendency of the predicted shear strength by different models to the varieties of the main design parameters (d , f'_c , ρ_f , E_f , a/d , and b_w). Generally, it can be observed that the proposed models, particularly the ANNs model, yielded larger shear capacities for all parameters, while ACI 440-15 yielded the lowest shear capacities which indicate that the ACI 440-15 is very conservative.

The relationship of beam depth with the predicted shear strength showed that all the proposed models and codes increased with the increase in the beam depth throughout the range of 100–1000 mm. The ACI 440-15 considers the effect of beam depth linearly, while all other models represent the effect of depth nonlinearly; the ANNs, GEP, and NLR models consider the depth raised to a power of 0.83, 0.67, and 0.66 respectively. Also, it can be observed that the GEP and NLR yield almost the same results. All the proposed models and codes showed an increase in shear strength with the increase in the concrete compressive

strength but in different rates. It was found that f'_c is raised to a power of 0.66, 0.30, and 0.2 for ANNs, GEP, and NLR, respectively.

The effect of the flexure reinforcement ratio on shear strength indicates a similar trend of the NLR model and the design codes, but the ANNs and GEP models showed a slightly decreased trend for reinforcement ratios greater than 0.03; this is not in agreement with codes and previous studies because of that only few data were available with ρ_f larger than 0.03, and these data actually showed decreasing shear capacity. Additionally, these models were derived based only on the artificial technology of data training without manually choosing the general mathematical shape of the model, in contrary to the NLR model and design codes which was derived based on the theoretical or semiempirical criteria.

The shear strength also increased with the increase in the elastic modulus of the flexure reinforcement ratio. It can be observed that all models showed a similar trend line for the entire range of data, while the ANNs model showed an increased rate up to about 110 GPa, and then the increase rate reduced significantly; similar results also obtained by Bashir and Ashour [8]. On the contrary, the trend lines of the shear span to depth ratio are decreased for GEP and NLR models for the entire range of data; meanwhile for ANNs model, it decreases up to a/d of 5, and then it started to increase slightly. This behavior is in agreement with the few available experimental results [32, 52, 56] which were studied as a/d greater than 5. However, other codes do not consider the effect of a/d as the trend lines for ACI 440-15 and JSCE-97 are constant, while the CSA S806 trend line remains constant beyond the a/d value of 5. Finally, the effect of beam width on shear strength is linear as indicated by trend lines for all models except the ANNs model which showed a lower increase rate beyond 700 mm width.

To investigate how the proposed models consider the size effect on shear capacity, the same parametric data used for studying the beam depth are used. Figure 9 presents

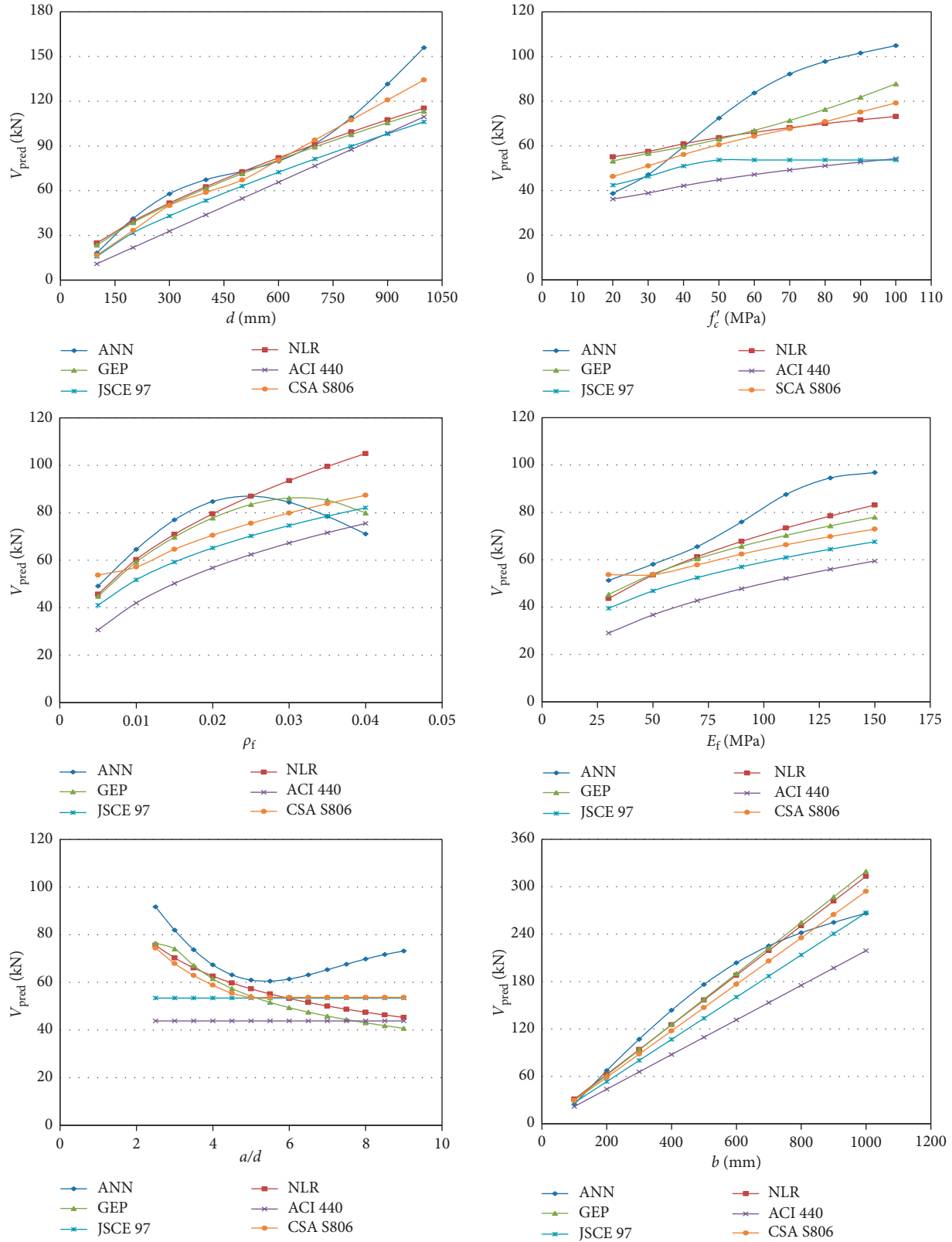


FIGURE 8: Effect of the parameters (d , f'_c , ρ_f , E_f , a/d , and b_w) on shear capacity predicted by ANNs, GEP, NLR, and three design codes (ACI.1R 440-06, JSCE-97, and CSA S806-12).

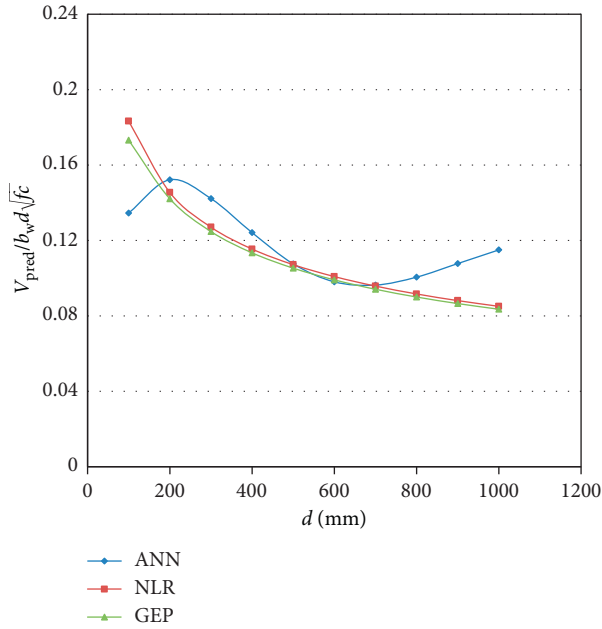


FIGURE 9: Normalized shear strength ($V_{pred}/b_w d \sqrt{f'_c}$) versus beam depth.

the relationship between normalized shear strength as ($V_{pred}/b_w d \sqrt{f'_c}$) and beam depth. It is clear that the normalized shear strength is decreased with the increase in the beam depth for ANNs, GEP, and NLR showing that the size effect is efficiently presented in these models. The trends of GEP and NLR are very close and compatible and decreased from a depth of 100 mm to 1000 mm, while the ANNs model seems to be more accurate as it shows an increase in the trend up to the depth of 200 mm, and then it decreased similarly to that of GEP and NLR; after that, the trend starts to increase slightly.

It can be summed up to that the artificial intelligent models, due to their efficiency and powerful ability in recognizing the parameters interaction, demonstrate various rates of change and fluctuation for the entire scope of input parameters. The ANNs and GEP models define accurately the interaction of each parameter on shear strength prediction and have a great ability to represent the actual response of each parameter in spite of its complexity and fluctuation nature. Furthermore, these models are evolved by training numerous preliminary linear and nonlinear models without any prior assumption regarding the shape and structure of the mathematical model.

9. Conclusions

An experimental database including 269 shear test results of FRP-reinforced concrete members without stirrups available in the literature was established to propose three prediction models to estimate the shear capacity of FRP-RC members using three powerful tools which are ANNs, GEP, and NLR. The following conclusions can be drawn from this study:

- (i) The proposed models for predicting the shear capacity of FRP-RC members based on ANNs and GEP techniques showed excellent performance, great efficiency, and high level of accuracy and yielded consistent results throughout a wide range of influencing parameters; moreover, the ANNs model is more superior than the GEP, as the SD and R^2 for ANNs are 0.113 and 0.9877 and for GEP are 0.162 and 0.97, respectively.
- (ii) A simple, rational, and yet accurate empirical equation was proposed for predicting shear strength of FRP-RC members by NLR. The equation considers all the important influencing parameters and simplified to be easy for use. In addition, it gives consistent and accurate results with SD and R^2 of 0.173 and 0.95, respectively.
- (iii) Through a comparative statistical analysis for the proposed models with seven shear design codes and six proposed equations from the literature, it has been found that the most accurate and efficient models are ANNs and GEP and to a lower degree NLR. Among the codes and available proposals, the CSA S806-12 and Ashour and Kara [20] equations were appearing to be more accurate than the others.
- (iv) From a parametric study considering all the influencing parameters on shear capacity, it was found that the ANNs model, and to a lower level GEP model, defines accurately the interaction of each parameter on shear capacity prediction and has a great ability to represent the actual response of each parameter in spite of its complexity and fluctuation nature.
- (v) The ANNs and GEP models demonstrate that the effect of flexure reinforcement ratio on shear capacity decreased beyond 0.03, as a real response to the available few data in this range; therefore, more studies are needed to confirm this case.
- (vi) The ANNs model demonstrated that the effect of a/d does not absolutely reduce the shear capacity, while beyond the a/d value of 5, its effect could become reverse and contribute to increase in the shear capacity as confirmed by few previous studies.
- (vii) The size effect is considered properly by the proposed models, particularly the ANNs model, which yields more accurate shear capacity prediction to the experimental results.

Data Availability

The (database of shear strength of beams without stirrups) data used to support the findings of this study are included within the article.

Conflicts of Interest

The authors declare that they have no conflicts of interest.

References

- [1] M. S. Alam and A. Hussein, "Size effect on shear strength of FRP reinforced concrete beams without stirrups," *Journal of Composites for Construction*, vol. 17, no. 4, pp. 507–516, 2013.
- [2] J. R. Yost, S. P. Gross, and D. W. Dinehart, "Shear strength of normal strength concrete beams reinforced with deformed GFRP bars," *Journal of Composites for Construction*, vol. 5, no. 4, pp. 268–275, 2001.
- [3] A. G. Razaqpur, B. O. Isgor, S. Greenaway, and A. Selley, "Concrete contribution to the shear resistance of fiber reinforced polymer reinforced concrete members," *Journal of Composites for Construction*, vol. 8, no. 5, pp. 452–460, 2004.
- [4] M. Nehdi, H. El Chabib, and A. A. Saïd, "Proposed shear design equations for FRP-reinforced concrete beams based on genetic algorithms approach," *Journal of Materials in Civil Engineering*, vol. 19, no. 12, pp. 1033–1042, 2007.
- [5] ASCE-ACI.445, "Recent approaches to shear design of structural concrete," *Journal of Structural Engineering*, vol. 124, no. 12, pp. 1375–1417, 1998.
- [6] R. Park and T. Paulay, *Reinforced Concrete Structures*, John Wiley & Sons, Hoboken, NJ, USA, 1975.
- [7] I. F. Kara, "Prediction of shear strength of FRP-reinforced concrete beams without stirrups based on genetic programming," *Advances in Engineering Software*, vol. 42, no. 6, pp. 295–304, 2011.
- [8] R. Bashir and A. Ashour, "Neural network modelling for shear strength of concrete members reinforced with FRP bars," *Composites Part B: Engineering*, vol. 43, no. 8, pp. 3198–3207, 2012.
- [9] K. Nasrollahzadeh and M. M. Basiri, "Prediction of shear strength of FRP reinforced concrete beams using fuzzy inference system," *Expert Systems with Applications*, vol. 41, no. 4, pp. 1006–1020, 2014.
- [10] S. Lee and C. Lee, "Prediction of shear strength of FRP-reinforced concrete flexural members without stirrups using artificial neural networks," *Engineering Structures*, vol. 61, pp. 99–112, 2014.
- [11] E. M. Golafshani and A. Ashour, "A feasibility study of BBP for predicting shear capacity of FRP reinforced concrete beams without stirrups," *Advances in Engineering Software*, vol. 97, pp. 29–39, 2016.
- [12] ACI-440, *Guide for the Design and Construction of Structural Concrete Reinforced with Fiber-Reinforced Polymer (FRP)*, ACI 440. 1R-15, American Concrete Institute, Farmington Hills, MI, USA, 2015.
- [13] JSCE, "Recommendation for design and construction of concrete structures using continuous fiber reinforcing materials," in *Concrete Engineering Series 23*, A. Machida, Ed., Japan Society of Civil Engineers, Tokyo, Japan, 1997.
- [14] BISE, *Interim Guidance on the Design of Reinforced Concrete Structures Using Fiber Composite Reinforcement*, British Institution of Structural Engineers, Seto, Ltd., London, UK, 1999.
- [15] CSA, Canadian Highway Bridge, *Design Code. Supplement No. 1 to CAN/CSA S6-06 (S6.1S1-10)*, Canadian Standards Association (CSA), Mississauga, ON, Canada, 2010.
- [16] ISIS, *Reinforced Concrete Structures with Fibre Reinforced Polymers—Design Manual No. 3*, University of Manitoba, ISIS Canada Corporation, Winnipeg, MB, Canada, 2007.
- [17] CNR-DT.203, "Guide for the design and construction of concrete structures reinforced with fiber-reinforced polymer bars," in *Advisory Committee on Technical Recommendations for Construction*, CNR-DT 203/2006, CNR, Rome, Italy, 2007.
- [18] CSA, "Code for the design and construction of building structures with fibre-reinforced polymers," in *CAN/CSA/S806-12*, p. 198, Canadian Standard Association, Toronto, ON, Canada, 2012.
- [19] A. Razaqpur and S. Spadea, "Resistenza a taglio di elementi di calcestruzzo rinforzati e staffe di FRP," in *Proceedings of AIAS*, Maratea, Italy, September 2010.
- [20] A. F. Ashour and I. F. Kara, "Size effect on shear strength of FRP reinforced concrete beams," *Composites Part B: Engineering*, vol. 60, pp. 612–620, 2014.
- [21] A. R. Yousif, "Shear strength of large FRP-reinforced concrete beams without shear reinforcement," *Journal of Pure and Applied Sciences*, vol. 27, pp. 9–28, 2015.
- [22] A. K. El-Sayed, E. F. El-Salakawy, and B. Benmokrane, "Shear capacity of high-strength concrete beams reinforced with FRP bars," *ACI Structural Journal*, vol. 103, p. 383, 2006.
- [23] A. G. Razaqpur and O. B. Isgor, "Proposed shear design method for FRP-reinforced concrete members without stirrups," *ACI Structural Journal*, vol. 103, p. 93, 2006.
- [24] K. Maruyama and W. Zhao, "Flexural and shear behaviour of concrete beams reinforced with FRP rods," in *Proceedings of the International Conference on Corrosion and Corrosion Protection of Steel in Concrete*, pp. 24–28, Sheffield, UK, 1994.
- [25] W. Zhao, K. Maruyama, and H. Suzuki, "Shear behavior of concrete beams reinforced by FRP rods as longitudinal and shear reinforcement," in *Proceedings of the Second International RILEM Symposium on Non-Metallic (FRP) Reinforcement for Concrete Structures*, p. 352, Ghent, Belgium, August 1995.
- [26] H. Nakamura and T. Higai, "Evaluation of shear strength of the concrete beams reinforced with FRP," in *Proceedings of Japan Society of Civil Engineers*, p. 89, Ghent, Belgium, 1995.
- [27] K. Maruyama and W. Zhao, "Size effect in shear behavior of FRP reinforced concrete beam," in *Advanced Composite Materials in Bridges and Structures*, pp. 227–234, Canadian Society for Civil Engineering, Montreal, QC, Canada, 1996.
- [28] Y. Mizukawa, Y. Sato, T. Ueda, and Y. Kakuta, "A study on shear fatigue behavior of concrete beams with FRP rods," in *Proceedings of the Third International Symposium on Non-Metallic (FRP) Reinforcement for Concrete Structures (FRPRCS-3)*, pp. 309–316, Japan Concrete Institute, Sapporo, Japan, 1997.
- [29] N. Duranovic, K. Pilakoutas, and P. Waldron, "Tests on concrete beams reinforced with glass fibre reinforced plastic bars," in *Proceedings of the Third International Symposium on Non-Metallic (FRP) Reinforcement for Concrete Structures (FRPRCS-3)*, pp. 479–486, Sapporo, Japan, 1997.
- [30] N. Swamy and M. Aburawi, "Structural implications of using GFRP bars as concrete reinforcement," in *Proceedings of 3rd International Symposium, FRPRCS*, pp. 503–510, Sapporo, Japan, 1997.
- [31] C. R. Michaluk, S. H. Rizkalla, G. Tadros, and B. Benmokrane, "Flexural behavior of one-way concrete slabs reinforced by fiber reinforced plastic reinforcements," *ACI Structural Journal*, vol. 95, pp. 353–365, 1998.
- [32] D. Deitz, I. Harik, and H. Gesund, "One-way slabs reinforced with glass fiber reinforced polymer reinforcing bars," *Special Publication*, vol. 188, pp. 279–286, 1999.
- [33] T. Alkhrdaji, M. Wideman, A. Belarbi, and A. Nanni, "Shear strength of GFRP RC beams and slabs," in *Proceedings of the*

- International Conference, Composites in Construction-CCC*, pp. 409–414, Porto, Portugal, 2001.
- [34] G. S. Melo and J. A. Rayol, "Shear resistance of GFRP reinforced concrete beams," in *Proceedings of the Rehabilitating and Repairing the Buildings and Bridges of Americas: Hemispheric Workshop on Future Directions*, Mayagüez, PR, USA, pp. 47–64, 2002.
- [35] A. K. Tureyen and R. J. Frosch, "Shear tests of FRP-reinforced concrete beams without stirrups," *ACI Structural Journal*, vol. 99, pp. 427–434, 2002.
- [36] S. P. Gross, J. R. Yost, D. W. Dinehart, E. Svensen, and N. Liu, "Shear strength of normal and high strength concrete beams reinforced with GFRP bars," in *Proceedings of International Conference on High Performance Materials in Bridges*, pp. 426–437, ASCE, Reston, VA, USA, 2003.
- [37] M. Tariq and J. Newhook, "Shear testing of FRP reinforced concrete without transverse reinforcement," in *Proceedings of Annual Conference of the Canadian Society for Civil Engineering*, pp. 1330–1339, Moncton, NB, Canada, June 2003.
- [38] S. Gross, D. Dinehart, J. Yost, and P. Theisz, "Experimental tests of high-strength concrete beams reinforced with CFRP bars," in *Proceedings of the 4th International Conference on Advanced Composite Materials in Bridges and Structures (ACMBS-4)*, Calgary, AB, Canada, 2004.
- [39] A. Lubell, T. Sherwood, E. Bentz, and M. P. Collins, "Safe shear design of large, wide beams: adding shear reinforcement is recommended," *Concrete International*, vol. 26, pp. 66–78, 2004.
- [40] J. Yost, S. Gross, G. Masone, and P. Hamelin, "Sustained load effects on deflection and ultimate strength of concrete beams reinforced with GFRP," in *Proceedings of the International Conference, Composites in Construction (CCC2005)*, Lyon, France, July 2005.
- [41] A. El-Sayed, E. El-Salakawy, and B. Benmokrane, "Shear strength of one-way concrete slabs reinforced with fiber-reinforced polymer composite bars," *Journal of Composites for Construction*, vol. 9, no. 2, pp. 147–157, 2005.
- [42] A. E. Kilpatrick and L. Easden, "Shear capacity of GFRP reinforced high strength concrete slabs," in *Proceedings of the 18th Australasian Conference on the Mechanics of Structures and Materials, Perth, Australia*, vol. 1, pp. 119–124, Taylor & Francis, London, UK, 2005.
- [43] A. K. El-Sayed, E. F. El-Salakawy, and B. Benmokrane, "Shear strength of FRP-reinforced concrete beams without transverse reinforcement," *ACI Structural Journal*, vol. 103, p. 235, 2006.
- [44] A. Ashour, "Flexural and shear capacities of concrete beams reinforced with GFRP bars," *Construction and Building Materials*, vol. 20, no. 10, pp. 1005–1015, 2006.
- [45] M. Guadagnini, K. Pilakoutas, and P. Waldron, "Shear resistance of FRP RC beams: experimental study," *Journal of Composites for Construction*, vol. 10, no. 6, pp. 464–473, 2006.
- [46] R. Dawborn and A. Kilpatrick, *Flexural Shear Capacity of High Strength Concrete Slabs Reinforced with Longitudinal GFRP Bars*, 2006.
- [47] J. Niewels, "Zum Tragverhalten von Betonbauteilen mit Faserverbundkunststoffbewehrung," Rheinisch-Westfälische Technische Hochschule Aachen, Lehrstuhl und Institut für Massivbau, Dissertation, 2008.
- [48] A. El-Sayed, K. Soudki, and E. Kling, "Flexural behaviour of self-consolidating concrete slabs reinforced with GFRP bars," in *Proceedings of the 9th International Symposium on Fiber Reinforced Polymer Reinforcement for Reinforced Concrete Structures*, pp. 13–15, Sydney, NSW, Australia, 2009.
- [49] A. Caporale and R. Luciano, "Indagine sperimentale e numerica sulla resistenza a taglio di travi di calcestruzzo armate con barre di GFRP," in *Proceedings of XXXVIII Convegno Nazionale AIAS*, Turin, Italy, September 2009.
- [50] R. Olivito and F. Zuccarello, "On the shear behaviour of concrete beams reinforced by carbon fibre-reinforced polymer bars: an experimental investigation by means of acoustic emission technique," *Strain*, vol. 46, no. 5, pp. 470–481, 2010.
- [51] E. C. Bentz, L. Massam, and M. P. Collins, "Shear strength of large concrete members with FRP reinforcement," *Journal of Composites for Construction*, vol. 14, no. 6, pp. 637–646, 2010.
- [52] A. G. Razaqpur, M. Shedid, and B. Isgor, "Shear strength of fiber-reinforced polymer reinforced concrete beams subject to unsymmetric loading," *Journal of Composites for Construction*, vol. 15, no. 4, pp. 500–512, 2011.
- [53] M. Alam and A. Hussein, "Effect of member depth on shear strength of high-strength fiber-reinforced polymer-reinforced concrete beams," *Journal of Composites for Construction*, vol. 16, no. 2, pp. 119–126, 2012.
- [54] F. Matta, A. K. El-Sayed, A. Nanni, and B. Benmokrane, "Size effect on concrete shear strength in beams reinforced with fiber-reinforced polymer bars," *ACI Structural Journal*, vol. 110-S50, pp. 617–628, 2013.
- [55] B. Abdul-Salam, A. Farghaly, and B. Benmokrane, "Evaluation of shear behavior for one-way concrete slabs reinforced with carbon-FRP bars," *GEN*, vol. 243, p. 1, 2013.
- [56] C. H. Kim and H. S. Jang, "Concrete shear strength of normal and lightweight concrete beams reinforced with FRP bars," *Journal of Composites for Construction*, vol. 18, no. 2, article 04013038, 2014.
- [57] D. Tomlinson and A. Fam, "Performance of concrete beams reinforced with basalt FRP for flexure and shear," *Journal of Composites for Construction*, vol. 19, no. 2, article 04014036, 2014.
- [58] M. A. Issa, T. Ovitigala, and M. Ibrahim, "Shear behavior of basalt fiber reinforced concrete beams with and without basalt FRP stirrups," *Journal of Composites for Construction*, vol. 20, no. 4, article 04015083, 2015.
- [59] A. El Refai and F. Abed, "Concrete contribution to shear strength of beams reinforced with basalt fiber-reinforced bars," *Journal of Composites for Construction*, vol. 20, no. 4, article 04015082, 2015.
- [60] G. B. Jumaa and A. R. Yuosif, "Size effect in shear failure of high strength concrete beams without stirrups reinforced with basalt FRP bars," *KSCE Journal of Civil Engineering*, 2018, In press.
- [61] M. T. Hagan, H. B. Demuth, and M. H. Beale, *Neural Network Design (Electrical Engineering)*, Thomson Learning, Boston, MA, USA, 1995.
- [62] S. S. Haykin, S. S. Haykin, S. S. Haykin, and S. S. Haykin, *Neural Networks and Learning Machines*, Pearson, Vol. 3, Pearson, Upper Saddle River, NJ, USA, 2009.
- [63] M. Y. Mansour, M. Dicleli, J.-Y. Lee, and J. Zhang, "Predicting the shear strength of reinforced concrete beams using artificial neural networks," *Engineering Structures*, vol. 26, no. 6, pp. 781–799, 2004.
- [64] H. Demuth, M. Beale, and M. Hagan, *Neural Network Toolbox™ 6, User's Guide*, The MathWorks, Inc., vol. 10, p. 11, Natick, MA, USA, 2008.
- [65] A. W. Oreta and K. Kawashima, "Neural network modeling of confined compressive strength and strain of circular concrete columns," *Journal of Structural Engineering*, vol. 129, no. 4, pp. 554–561, 2003.

- [66] S. Jung and K. S. Kim, "Knowledge-based prediction of shear strength of concrete beams without shear reinforcement," *Engineering Structures*, vol. 30, no. 6, pp. 1515–1525, 2008.
- [67] Z.-H. Duan, S.-C. Kou, and C.-S. Poon, "Prediction of compressive strength of recycled aggregate concrete using artificial neural networks," *Construction and Building Materials*, vol. 40, pp. 1200–1206, 2013.
- [68] H. El-Chabib, M. Nehdi, and A. Said, "Predicting shear capacity of NSC and HSC slender beams without stirrups using artificial intelligence," *Computers and Concrete*, vol. 2, no. 1, pp. 79–96, 2005.
- [69] F. Altun, Ö. Kişi, and K. Aydin, "Predicting the compressive strength of steel fiber added lightweight concrete using neural network," *Computational Materials Science*, vol. 42, no. 2, pp. 259–265, 2008.
- [70] J. R. Koza, "Genetic programming as a means for programming computers by natural selection," *Statistics and Computing*, vol. 4, no. 2, pp. 87–112, 1994.
- [71] C. Ferreira, "Gene expression programming in problem solving," in *Soft Computing and Industry*, pp. 635–653, Springer, Berlin, Germany, 2002.
- [72] C. Kayadelen, "Soil liquefaction modeling by genetic expression programming and neuro-fuzzy," *Expert Systems with Applications*, vol. 38, no. 4, pp. 4080–4087, 2011.
- [73] A. H. Gandomi, A. H. Alavi, and G. J. Yun, "Formulation of uplift capacity of suction caissons using multi expression programming," *KSCE Journal of Civil Engineering*, vol. 15, no. 2, pp. 363–373, 2011.
- [74] A. H. Gandomi, A. H. Alavi, and C. Ryan, *Handbook of Genetic Programming Applications*, Springer, Berlin, Germany, 2015.
- [75] A. H. Gandomi and A. H. Alavi, "A new multi-gene genetic programming approach to non-linear system modeling. Part II: geotechnical and earthquake engineering problems," *Neural Computing and Applications*, vol. 21, no. 1, pp. 189–201, 2012.
- [76] A. H. Alavi and A. H. Gandomi, "Energy-based numerical models for assessment of soil liquefaction," *Geoscience Frontiers*, vol. 3, no. 4, pp. 541–555, 2012.
- [77] L. Teodorescu and D. Sherwood, "High energy physics event selection with gene expression programming," *Computer Physics Communications*, vol. 178, no. 6, pp. 409–419, 2008.
- [78] GEPSOFT, *GeneXproTools, Version 5.0*, GEPSOFT, Bristol, UK, 2013, <http://www.gepssoft.com>.
- [79] S. M. Mousavi, P. Aminian, A. H. Gandomi, A. H. Alavi, and H. Bolandi, "A new predictive model for compressive strength of HPC using gene expression programming," *Advances in Engineering Software*, vol. 45, no. 1, pp. 105–114, 2012.
- [80] M. Saridemir, "Empirical modeling of splitting tensile strength from cylinder compressive strength of concrete by genetic programming," *Expert Systems with Applications*, vol. 38, no. 11, pp. 14257–14268, 2011.
- [81] M. Sonebi and A. Cevik, "Genetic programming based formulation for fresh and hardened properties of self-compacting concrete containing pulverised fuel ash," *Construction and Building Materials*, vol. 23, no. 7, pp. 2614–2622, 2009.
- [82] A. H. Alavi, P. Aminian, A. H. Gandomi, and M. A. Esmaili, "Genetic-based modeling of uplift capacity of suction caissons," *Expert Systems with Applications*, vol. 38, no. 10, pp. 12608–12618, 2011.
- [83] T. Zsutty, "Shear strength prediction for separate categories of simple beam tests," *ACI Journal Proceedings*, vol. 68, no. 2, pp. 138–143, 1971.

